2022-11

Liquid air energy storage for ancillary services in an integrated hybrid renewable system

Kheshti, M

10.1016/j.renene.2022.09.010
Renewable Energy
Elsevier

Renewable Energy 199 (2022) 298–307

Contents lists available at ScienceDirect

Renewable Energy

journal homepage: www.elsevier.com/locate/renene

Liquid air energy storage for ancillary services in an integrated hybrid renewable system

Mostafa Kheshti [a], Xiaowei Zhao [a,*], Ting Liang [b], Binjian Nie [c], Yulong Ding [b], Deborah Greaves [d]

[a] Intelligent Control and Smart Energy (ICSE) Research Group, School of Engineering, University of Warwick, Coventry, CV4 7AL, UK
[b] Birmingham Centre for Energy Storage, School of Chemical Engineering, University of Birmingham, Birmingham, B15 2TT, UK
[c] Department of Engineering Science, University of Oxford, Parks Road, Oxford, OX1 3PJ, UK
[d] School of Engineering, Computing and Mathematics, University of Plymouth, Drake Circus, Plymouth, PL4 8AA, UK

ARTICLE INFO

Keywords:
ancillary service
Fast frequency response
Hybrid renewable sources
Liquid air energy storage
Microgrid
Wind energy

ABSTRACT

High shares of intermittent renewable sources cause volatile frequency movements that could jeopardize the continuous operation of the grid. Liquid Air Energy Storage (LAES) is an emerging technology that not only helps with decarbonisation of energy sectors, but also has potentials for reliable ancillary services. In this paper, a hybrid LAES, wind turbine (WT), and battery energy storage system (BESS) is used to investigate their contributions in fast frequency control. The inertial control, droop control and combined inertial and droop terms are applied on each source of the hybrid renewable system and a comprehensive analysis is conducted to study their impacts on the frequency nadir improvement. The analysis shows that LAES with combined inertial and droop control terms along with inertial control of WT and BESS provide reliable frequency control. To further improve the frequency nadir, a Fuzzy control is proposed and applied on the LAES. The proposed control system provides a more adaptive performance against disturbances. Also, experimental tests are conducted to validate the proposed control method using a real-time hardware-in-the-loop test rig. The simulation and experimental results show that LAES in a hybrid renewable system can significantly contribute to the frequency control when variable gain control schemes are implemented.

1. Introduction

With the emerging concerns on the global warming, there has been an unprecedented push towards decarbonisation. The UK government has set policies and commitments to decarbonise the UK electricity system by 2035. In this regard, the coal-based power plants will be phased out from the electricity network by October 2024 [1]. According to the British energy security strategy, 50 GW offshore wind power capacity will be accommodated into the electricity network, as well as production of 10 GW hydrogen by 2030, alongside large-scale and long-duration compressed air energy storage to achieve increased system flexibility [2]. Hybrid renewable energy sources (RES) have been put into development and operation as the key enablers to reach net zero targets. Around 90% of the global power capacity expansion between 2021 and 2022 has come from renewables [3,4].

Large shares of RESs into the power system cause reduction in the system inertia, where grid frequency movements become more volatile and unpredictable [5,6]. In particular, where the power system is small or even in the microgrids, ancillary service support from hybrid RESs along with energy storage technologies is essentially required. Battery energy storage (BESS) as a competitive solution, provides fast power response and with short duration storage up to 4h [7]. However, they remain unfavourable due to high maintenance costs, short life cycle and degradation in performance with aging [8,9].

Other forms of maturely developed large-scale energy storage technologies such as pump hydro energy storages (PHES) [10] and compressed air energy storage (CAES) [11] are restrained by the geographical locations. For PHES, water will be stored in an elevated reservoir, it is the most widely adopted electrical storage technology due to its low cost (5–100 $/kWh), high efficiency and high technology readiness level [12], but is limited by geographical requirements. The compressed air energy storage requires underground caverns and costly high-pressure vessels, which has relatively high efficiency (up to 70%) with low cost (20–200 $/kWh) [17]. But these storages have low energy densities and require large storage volumes [27]. Therefore, low-cost, long-duration and geographically unconstrained grid-scale energy

* Corresponding author.
E-mail address: xiaowei.zhao@warwick.ac.uk (X. Zhao).

https://doi.org/10.1016/j.renene.2022.09.010
Received 7 June 2022; Received in revised form 29 August 2022; Accepted 2 September 2022
Available online 8 September 2022

storage solutions are in urgent need.

Liquid air energy storage (LAES) has been an attractive alternative to PHES and CAES due to its low cost, ease of deployment and scalability without geographical constraints. As the storage medium is liquid air, the tank size is considerably smaller, with reduced operational costs, higher energy density and better integration with other energy sources [28] to form a hybrid system. At present, most researchers have worked on the thermodynamic analysis and parametric studies of LAES. For example, Guizzi et al. [12] and Xue et al. [13] stated the round trip efficiency (RTE) of the stand-alone LAES can reach around 50% when the system operated under optimal thermodynamic conditions. She et al. [14] and Peng et al. [15] discussed the impacts of recoverable waste heat and cold energy on RTE, which can be improved to be around 60%. In Ref. [29], a preliminary study on the optimal configuration of a small microgrid scale air liquefaction cycle for LAES application was conducted, in order to minimize the specific consumption. LAES can also provide multiple benefits to the hybrid systems, including price arbitrage, peak shaving, renewable capacity firming, operating reserve and back-up power, as well as providing flexibility and other auxiliary services [16]. The research in Ref. [30] assessed the economic feasibility of LAES technology in the UK energy market and focused on the short-term operating reserve service provided by a stand-alone LAES system. Authors in Ref. [31] modelled and assessed the interdependence techno-economic performance of a LAES plant providing energy arbitrage and reserve services in the UK electricity market. The research in Ref. [32] presented the frequency response time characteristics of large-scale energy storage system in a high renewable integrated grid. Several researchers have worked on developing the control strategy of LAES based on the full dynamic model of LAES. A 10% of load step-down method and a combination control model were proposed by Guo et al. [17] to achieve shorter load balance time and smaller dynamic overshoot. Cui et al. [18] proposed that the control strategy design, and the sensitivity analysis of rotor speed rising rate and frequency disturbance can help expand the understanding of LAES and provide practical application guidance. The same authors [19] have developed the schemes for start-up and primary frequency regulation. Lu et al. [20] studied the impact of rotor time constant and valve closing time on the rotor speed and shutdown time of the LAES discharging unit. It is recommended that the rotor time constant should be less that 7s, the closing time of the control valve should not exceed 1.5s, to meet the safety requirements of the system.

Whilst there has been a progressive research on the efficiency enhancement and utilization of LAES in the energy mix, only very few attempts have been made to analyse its application for fast frequency response (FFR) in a low inertia system. Motivated to fill this gap and utilize the advantages of the LAES technology for power system frequency control as a new emerging renewable source, this paper develops a hybrid RES-based frequency control for microgrid applications, comprising LAES, battery energy storage (BESS) and variable speed wind turbine (WT). A Fuzzy-based FFR scheme is developed that allows LAES to participate in frequency control upon occurring a disturbance. An autonomous inertial control system is also developed for the BESS and WT to contribute to the frequency control. The proposed control scheme of this hybrid renewable system is analysed in different scenarios.

The main novelties and contribution of this paper are as follows:

- A novel hybrid renewable energy-based scheme comprising LAES, WT, and BESS is proposed to participate in FFR and improve the frequency nadir against active power unbalances in a microgrid system.
- A Fuzzy control is proposed and developed to adaptively control the power output of LAES during frequency events. The grid frequency deviation and rate of change of frequency (ROCOF) are used as the input of this controller. The output of the controller is the active power reference of LAES.
- Inertial and droop control terms are applied on WT and BESS to provide FFR support. A comprehensive assessment on impact of inertial, droop and both inertial-droop control terms of the hybrid system on the frequency nadir is conducted. The impact of these control terms on secondary frequency dip (SFD) is also analysed. The comparison demonstrates the effectiveness of the proposed Fuzzy control of LAES along with the inertial control of WT and BESS on grid frequency nadir improvement.
- The proposed control scheme is tested on a microgrid system comprising PV, WT, BESS, LAES, diesel generation, and load. The control scheme is also validated using a real-time power hardware-in-the-loop experimental platform.

The remainder of the paper is organized as follows: in Section 2, the hybrid RES system is described in detail. The control strategy is explained in section 3. The proposed hybrid system and its novel control scheme are tested in Section 4, on a microgrid comprising PV, WT, LAES, BESS, loads and distributed generator, to provide a realistic and complex low inertia system scenario. The proposed system is validated using a state-of-the-art real-time hardware-in-the-loop test rig. In section 5, a discussion is presented on the economic and environmental aspect of LAES along with the future works. Finally, section 6 concludes the results of the paper.

2. Hybrid renewable energy system description

2.1. Liquid air energy storage

LAES is a kind of cryogenic energy storage that uses liquefied air or nitrogen as a storage medium [33]. The operation principle of LAES technology is divided into three processes, the charging, storage and discharging processes, as shown in Fig. 1. In the charging process, the surplus electrical power from the grid or RESs in the microgrid is used to purify the ambient air, compress and convert into liquid air by cooling it down. The liquefied air is then stored at low-pressure in an insulated tank. When the load demand in the grid increases or a frequency dip event occurs, the stored liquid air is pumped to high pressure and heated by waste heat for evaporation, which then drives the turbine and generates electricity. During the compression stage, the compression heat is stored in a hot storage tank, which can be used to superheat the air in the discharging process to increase power output. During the evaporation stage, the high-grade cold exergy is recovered and stored in cold storage tank, which can be reused in the cooling-down process, reducing power consumption at the charging system [34]. The harness and re-use of hot and cold thermal steams can significantly increase the plant efficiency.

2.1.1. Compressor model

A compressor train is used in LAES to increase the air pressure. The compression ratio for each stage is π_c [21].

$$\pi_c = \frac{P_{c,out}}{P_{c,in}} \tag{1}$$

where, symbol P – pressure, subscript c – compressor, in – inlet position, out – outlet position.

The efficiency η_c of compressors is expressed by empirical equation [21]:

$$\eta_c = 0.91 + \frac{\pi_c - 1}{300} \tag{2}$$

The outlet temperature of the compressor is $T_{c,out}$ [22]:

$$T_{c,out} = T_{in,c}\left(1 + \frac{1}{\eta_c}\left(\pi_c^{\frac{k-1}{k}} - 1\right)\right) \tag{3}$$

where, symbol T – temperature, k – adiabatic index.

The power consumption of the compressor is expressed as [22]:

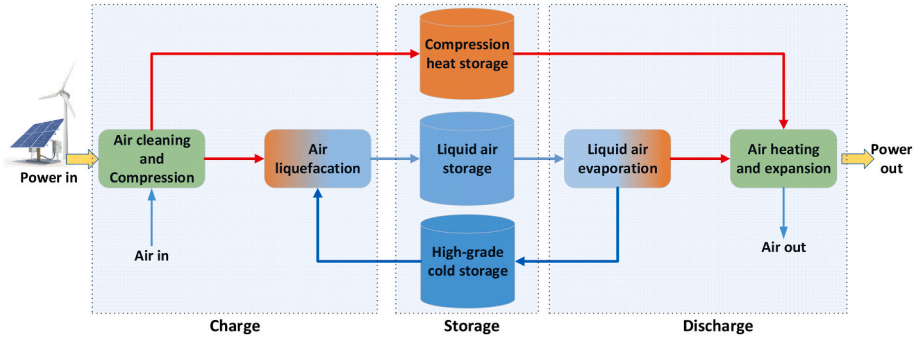

Fig. 1. Schematic diagram of the liquid air energy storage system.

$$P_{w,c} = \frac{1}{\eta_c} q_{mc} C_p T_{in,c} \left(\pi_c^{\frac{k-1}{k}} - 1 \right) \tag{4}$$

where, symbol P_w – power output, q_m – mass flow rate of fluid. C_p – specific heat capacity.

2.1.2. Turbine model

A turbine train is used in LAES to expand the air to produce power output. The expansion ratio for each stage is π_t [21].

$$\pi_t = \frac{P_{t,in}}{P_{t,out}} \tag{5}$$

where, subscript t – turbine.

The efficiency η_t of turbines is expressed by empirical equation [21]:

$$\eta_t = 0.9 - \frac{\pi_t - 1}{250} \tag{6}$$

The outlet temperature of compressor is $T_{t,out}$ [22]:

$$T_{t,out} = T_{in,t} \left(1 - \eta_t \left(1 - \pi_t^{\frac{1-k}{k}} \right) \right) \tag{7}$$

The power output $P_{w,t}$ of the turbine is expressed as [22]:

$$P_{w,t} = \eta_t q_{mt} C_p T_{in,t} \left(1 - \pi_t^{\frac{k-1}{k}} \right) \tag{8}$$

2.1.3. Heat exchanger model

The counter-flow heat exchangers (HEX) are widely adopted in LAES, including the coolers, heaters, cold boxes and evaporators. The HEX model can be expressed by the ε-NTU method [23]. ε is the heat transfer effectiveness. The NTU is around 10–14. C_R is a dimensionless parameter [23].

$$T_{a,out} = \varepsilon T_{m,in} + (1 - \varepsilon) T_{a,in} \tag{9}$$

$$T_{m,out} = \varepsilon T_{a,in} + (1 - \varepsilon) T_{m,in} \tag{10}$$

$$\varepsilon = \frac{1 - \exp[-NTU(1 - C_R)]}{1 - C_R \exp[-NTU(1 - C_R)]} \tag{11}$$

where, subscript a – air, m – another heat transfer fluid.

2.1.4. Pump model

The pump is modelled according to affinity law, which expresses the relationship between the pressure head and the mass flow rate, shown as the following. The efficiency of the pump is expressed by a second-order poly-nominal fitting equation [24].

$$\frac{\Delta P}{\Delta P_0} = \left(\frac{q_{m,p}}{q_{m,0p}} \right)^2 \tag{12}$$

where, δP – heat of pump, subscript 0 – the state at the rated conditions, p – pump.

2.2. Variable speed wind turbine

In normal operations, the WT operates at the maximum power point tracking (MPPT) to extract maximum power from the varying wind. The P_{mppt} is the electric power output of the machine in the MPPT mode that is a cubic function of the rotor speed, ω_r [38].

$$P_{mppt}(\omega_r) = k_{opt} \omega_r^3 \tag{13}$$

where k_{opt} is the constant controller gain and coefficient of the MPPT curve. The MPPT operation mode is at the maximum mechanical power extraction, formulated as follows [36,42]:

$$P_m = \frac{1}{2} \rho \pi r^2 C_p(\lambda, \beta) v_w^3 \tag{14}$$

$$C_p(\lambda, \beta) = 0.22 \left(\frac{116}{\lambda_i} - 0.4\beta - 5 \right) e^{\frac{-12.5}{\lambda_i}} \tag{15}$$

$$\frac{1}{\lambda_i} = \frac{1}{\lambda + 0.08\beta} - \frac{0.035}{\beta^3 + 1} \tag{16}$$

$$\lambda = \frac{r\omega_r}{v_w} \tag{17}$$

where ρ, r, λ, and β are the air density, blade radius, tip-speed ratio and the pitch angle, respectively. The maximum value of mechanical power P_m can be obtained by maximizing the function $C_p(\lambda, \beta)$, which is a nonlinear function of the tip-speed-ratio λ and the blade pitch angle β as formulated in (15)-(17) and illustrated in Fig. 2. The maximum mechanical power extraction is when the pitch angle $\beta = 0$.

The grid frequency is a dynamic response of mismatched balance between the generation and consumption. When a disturbance such as connection of a big load or disconnection of a large generator occurs, the frequency deviates from its nominal value. Considering the frequency response model of a power system [35], the frequency deviation at the time of disturbance, can be calculated as follows [36]:

$$\Delta f = = \left(\frac{R\Omega_n^2}{D_s R + K_m} \right) \left(\frac{(1 + T_R s) P_d}{s\left(s^2 + 2\zeta\Omega_n s + \Omega_n^2\right)} \right) \tag{18}$$

subject to

$$\Omega_n^2 = \frac{D_s R + K_m}{2 H_s R T_R} \tag{19}$$

$$\zeta = \left[\frac{2H_s R + (D_s R + K_m F_H) T_R}{2(D_s R + K_m)} \right] \Omega_n \tag{20}$$

where D_s presents the grid damping factor; K_m is mechanical power gain factor; R refers to the regulation factor of the governor; F_H is the fraction of total power generated by the HP turbine; H_s is the system inertia

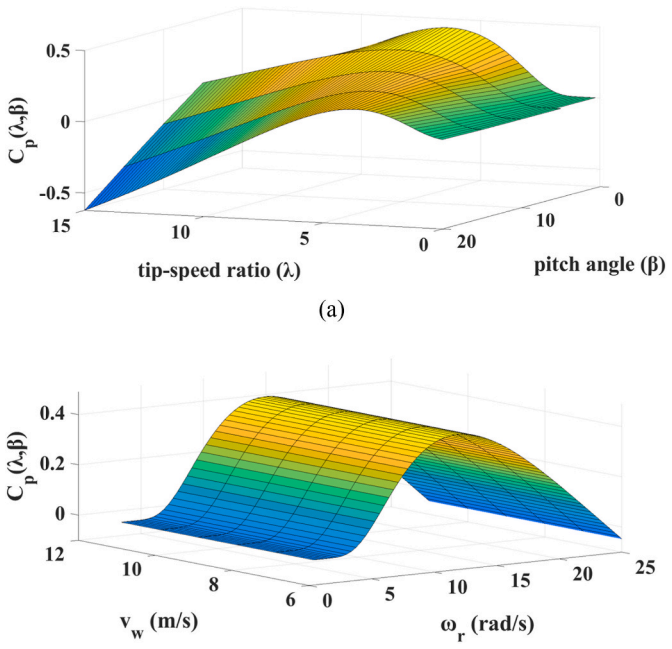

Fig. 2. Aerodynamic performance of a wind turbine. (a) as a function of λ_i and β (b) as a function of v_w and ω_r when $\beta = 0$.

constant; T_R is the reheat time constant. P_d is the disturbance that causes frequency deviation [35,36].

The time domain presentation of the frequency deviation, is the inverse Laplace Transform of (18), which is formulated as [35]:

$$\Delta f(t) = \frac{RP_d}{D_s R + K_m}\left[1 + \alpha e^{-\zeta\Omega_n t}\sin(\Omega_r t + \varphi)\right] \tag{21}$$

where,

$$\Omega_r = \Omega_n\sqrt{1-\zeta^2} \tag{22}$$

$$\alpha = \sqrt{\frac{1 - 2T_R\zeta\Omega_n + T_R^2\Omega_n^2}{1-\zeta^2}} \tag{23}$$

$$\varphi = \varphi_2 - \varphi_1 = \arctan\left(\frac{\Omega_r T_R}{1-\zeta\Omega_n T_R}\right) - \arctan\left(\frac{\sqrt{1-\zeta^2}}{-\zeta}\right) \tag{24}$$

At the instance of the disturbance event ($t = 0$), the df/dt has the largest magnitude, while it becomes smaller till the frequency arrives to its nadir, in which $df/dt = 0$ [35].

$$\left.\frac{d\Delta f}{dt}\right|_{t=0} = \left.\frac{\alpha\Omega_n RP_d}{2\pi(D_s R + K_m)} e^{-\zeta\Omega_n t}\sin(\Omega_r t + \varphi_1)\right|_{t=0} = \frac{P_d}{2H_s} \tag{25}$$

2.3. Battery energy storage

For a Li-ion battery, the charge model is modelled as [25,26]:

$$E_{t,cha} = E_0 - K\cdot\frac{Q_{max}}{Q_t + 0.1\cdot Q_{max}}\cdot I_{low} - K\cdot\frac{Q_{max}}{Q_{max} - Q_t}\cdot Q_t + A\cdot e^{(-B\cdot Q_t)} \tag{26}$$

The discharge model is formulated as [25,26]:

$$E_{t,dis} = E_0 - K\cdot\frac{Q_{max}}{Q_{max} - Q_t}\cdot I_{low} - K\cdot\frac{Q_{max}}{Q_{max} - Q_t}\cdot Q_t + A\cdot e^{(-B\cdot Q_t)} \tag{27}$$

where, E_0-the constant voltage, V. Q_{max} - the maximum capacity, Ah. K – the polarization constant, V/Ah. Q_t – the extracted capacity, Ah. Symbol A - exponential voltage, in V. B is the exponential capacity, in Ah^{-1}. I_{low} – low frequency current dynamics, A. E_t- voltage at time t. subscript *cha*- charging process, *dis* – discharging process.

3. Fast Frequency Response Control strategy

3.1. Inertial-droop control scheme

Frequency of a power system is an indication of how balanced the power generation and demand are. When the total generation power P_{gen} is equal to the total consumption power P_{load}, the grid frequency is at its nominal value. When a frequency event occurs, such as disconnection of a large generator or connection of high loads, the synchronously connected generators and motors will naturally rotate slower by releasing a portion of their kinetic energy into the grid, corresponding to the size of the disturbance. The change in the frequency should always be kept small within the statutory limits to maintain the operation of the connected appliances as well as ensuring the stability of the entire system. In this context, the frequency changes are small around the nominal value (e.g. 50 Hz or 60 Hz) and the frequency drop is formulated as [37]:

$$\frac{dE_{KE}}{dt} \approx Jf_0\frac{df}{dt} \approx P_{gen} - P_{load} \tag{28}$$

where, E_{KE} denotes the stored kinetic energy of the rotating masses, synchronously connected to the grid, f is the grid frequency with its nominal value presented by f_0. The total system inertia is shown by J. To respond to a frequency event, the mechanical inputs of synchronous generators need to change via governor action. As the mechanical responses are slow, the changes in P_{gen} do not instantaneously happen. Therefore, the system inertia J determines the initial frequency movements. This inertial response is critical to stabilize the grid frequency. Larger J directly improves the frequency nadir and limits ROCOF, providing a momentum to the primary frequency control to counterbalance the frequency.

With higher shares of intermittent renewable sources such as wind, the total system inertia decreases, causing a more volatile frequency movement, sensitive to disturbances. WTs are decoupled from the grid due to the power electronics converter interfaces and do not naturally participate in frequency control. There are two main strategies for WTs to provide fast frequency response. The stepwise inertial control approaches [38,39] and the frequency-based methods [40,41]. The stepwise methods immediately inject a predefined active power to the grid by extracting all or a portion of their stored kinetic energy in the rotating mass. However, in these schemes, to avoid the over-deceleration of rotor speed, the overproduction terminates in ramp-like or stepwise form, imposing an SFD that may jeopardize the grid stability.

The frequency-based methods emulate the natural behaviour of synchronous generators, by measuring the frequency and its change to proportionally provide active power to the grid. The control scheme is shown in Fig. 3.

When a large active power event occurs in the system, the frequency deviates from its steady state, and an additional inertial response, proportional to the derivative of the frequency is added to the output power

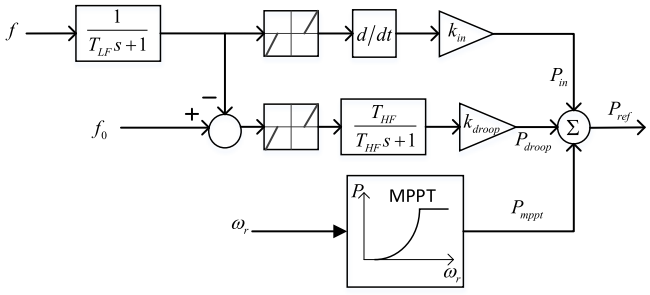

Fig. 3. Inertia emulation and droop control scheme.

of WT.

The inertial response can be interpreted as the injection of active power, proportional to the size of ROCOF [37]:

$$P_{in} = -k_{in}\frac{df}{dt} \tag{29}$$

To bypass the measurement noise in the frequency, a low-pass filter is used. It is important to finely adjust such filter as the differentiation operation on a noisy signal may lead to undesired torque pulsation in the WT drive train. Also, a dead-band is assigned to avoid the activation of the inertial response loop against small load changes.

Complementary to the inertial response loop, a droop term is added, proportional to the frequency deviation ($\Delta f = f\text{-}f_0$). At the instance of the frequency event, the deviation from the nominal frequency f_0 is small until it arrives at the frequency nadir, where the frequency deviation is largest. Therefore, the contribution of the droop term is small at the beginning and large when arriving at the frequency nadir, formulated as follows [37]:

$$P_{droop} = -k_{droop}\Delta f \tag{30}$$

To ensure that the droop term of the WT does not operate at the steady state, and allowing the rotor speed recovery to its previous working point, a high-pass filter is added. However, the proper parameter tuning of the high-pass filter shown by T_{HF}, is essential. Adding both droop and inertial response terms, the final reference power for the wind turbine is [37]:

$$P_{ref} = P_{mppt} + P_{in} + P_{droop} = P_{mppt} - k_{in}\frac{df}{dt} - k_{droop}\Delta f \tag{31}$$

3.2. Fuzzy-based FFR from LAES

Application of Fuzzy control has been widely investigated in the open literature, thanks to its robustness, simplicity and being independent of the detailed mathematical model of a system. Fuzzy control methods use the expert's knowledge on the dynamics of a system to develop the controller based on *if-then* sets of relationships between the inputs and outputs of that system. Three building blocks of this controller are Fuzzification, Fuzzy Interference System, and Defuzzification.

In the Fuzzification step, the input/output signals are described with the linguistic membership functions. In this paper, three linguistics variables are used, namely N (negative), Z (zero), P (positive), as shown in Fig. 4. The frequency deviation and its derivative are the two inputs of the Fuzzy controller. The output signal is the power reference sent to LAES to provide ancillary service and to counterbalance the frequency.

Fuzzy Inference is the process of mapping the inputs to the outputs, using the *if-then* rule based relationships. The *Mamdani*-type Fuzzy Inference System has been used for this purpose and the Fuzzy rules are presented in Table 1. To Defuzzify the linguistic rules into a crisp executable number, the *Centre of Area* (COA) is used. The centre of gravity of the final fuzzy space is calculated and executed by COA.

The LAES, WT and BESS provide fast dynamic responses for ancillary services. In this paper, The LAES uses Fuzzy controller to adaptively respond to the frequency events. The WT and the BESS use the emulated inertial response control to contribute to the frequency response.

4. Simulation and experimental results

4.1. Simulation results

In this section a microgrid system is used to verify the performance of the proposed control scheme for the fast frequency response capability. The microgrid system is shown in Fig. 5 and comprises a hybrid renewable energy system of 8 MW PV plant, 10 MW full-scale converter WT, 10 MW LAES, 5 MW BESS. The diesel generator has 15 MW capacity

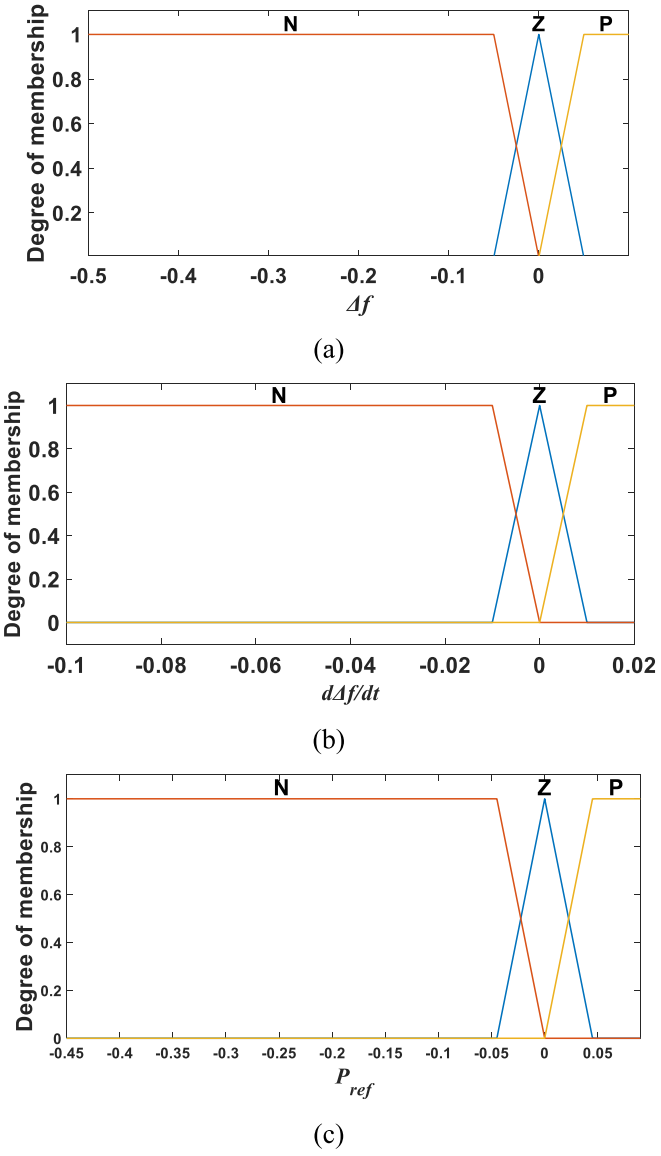

Fig. 4. Fuzzy control scheme of LAES (a) frequency deviation as input1 (b) ROCOF as input2 (a) Reference power as output signal.

Table 1
Input-Output Fuzzy relationships of LAES fast frequency response scheme.

	$d\Delta f/dt$		
Δf	**N**	**Z**	**P**
N	N	Z	P
Z	N	Z	P
P	N	P	P

while the load is 50 MW. The microgrid is connected to the upper stream grid. At t = 5s, it is disconnected from the grid to provide a realistic power imbalance event.

Firstly, the hybrid LAES-WT-BESS system operates with the inertial response control. The inertial control system has three operation possibilities, inertia term only, droop term only, or both inertia and droop loops. Having three resources of LAES, WT and BESS, therefore, there are 27 different control scenarios. Table 2 presents these scenarios and their performance on the frequency response. The frequency nadir at each case is considered the criteria to evaluate the FFR capability of these scenarios. Fig. 6 (a) shows the performance of 27 FFR schemes.

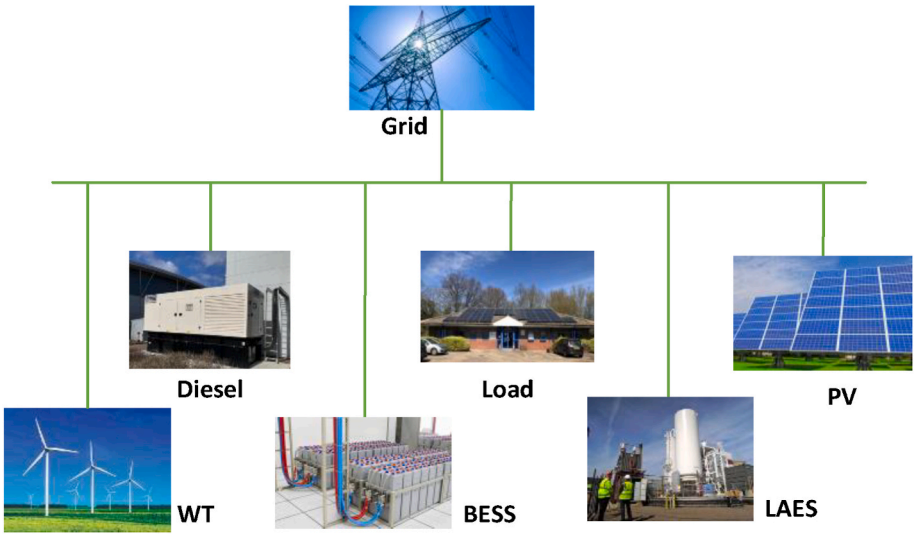

Fig. 5. Integrated hybrid renewable energy system as the case study.

Table 2
Different control scheme scenarios implemented on the hybrid LAES-WT-BESS.

Case no.	WT	LAES	BESS	Frequency Nadir (Hz)
1	inertia	inertia	inertia	59.526
2	inertia	inertia	droop	59.526
3	inertia	inertia	inertia-droop	59.526
4	inertia	droop	inertia	59.754
5	inertia	droop	droop	59.754
6	inertia	droop	inertia-droop	59.754
7	inertia	inertia-droop	inertia	59.754
8	inertia	inertia-droop	droop	59.754
9	inertia	inertia-droop	inertia-droop	59.754
10	droop	inertia	inertia	59.685
11	droop	inertia	droop	59.685
12	droop	inertia	inertia-droop	59.685
13	droop	droop	inertia	59.524
14	droop	droop	droop	59.521
15	droop	droop	inertia-droop	59.521
16	droop	inertia-droop	inertia	59.577
17	droop	inertia-droop	droop	59.574
18	droop	inertia-droop	inertia-droop	59.574
19	inertia-droop	inertia	inertia	59.701
20	inertia-droop	inertia	droop	59.702
21	inertia-droop	inertia	inertia-droop	59.702
22	inertia-droop	droop	inertia	59.543
23	inertia-droop	droop	droop	59.544
24	inertia-droop	droop	inertia-droop	59.544
25	inertia-droop	inertia-droop	inertia	59.587
26	inertia-droop	inertia-droop	droop	59.585
27	inertia-droop	inertia-droop	inertia-droop	59.585

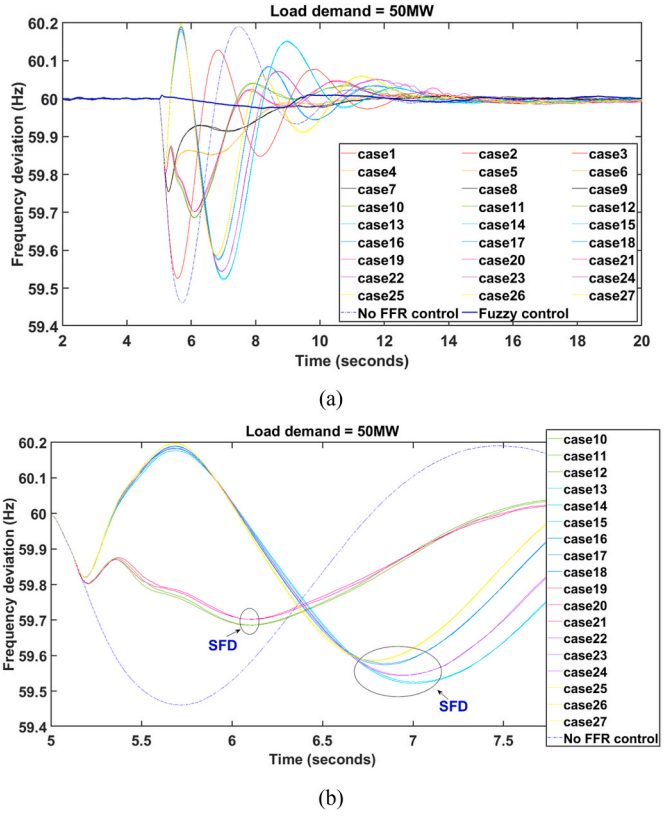

Fig. 6. Fast Frequency Response Control in the microgrid (a) different control scenarios of hybrid LAES-Wind-BESS system on frequency nadir (b) SFD effects of the corresponding control cases.

The labelled case number in the figure refers to the Table 2. For example, case no. 20 means the FFR controller scheme in which the WT is working at both inertia-droop terms, LAES controller is working at inertia term only, while the BESS is operating with the droop term only.

It can be seen that when the hybrid system operates with the case 7 (WT provides inertia only, LAES provides both inertia-droop; BESS with inertia only) frequency nadir is at its high point of 59.754 Hz. The responses from the hybrid system are shown in Figs. 7–9. LAES is capable of storing energy with longer period, more energy density and less space

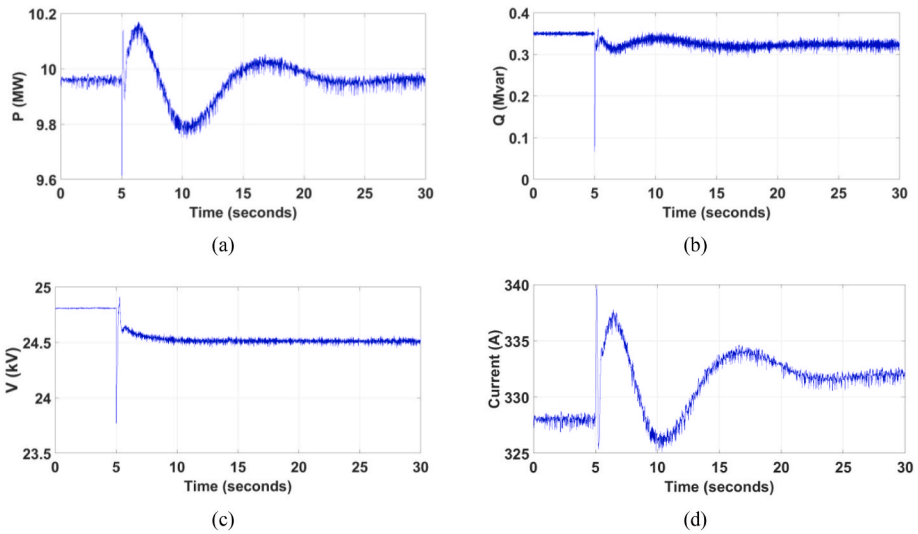

Fig. 7. Response of the WT against microgrid disconnection (a) active power response (b) reactive power response (c) voltage at the access point (d) Current waveform response of the WT.

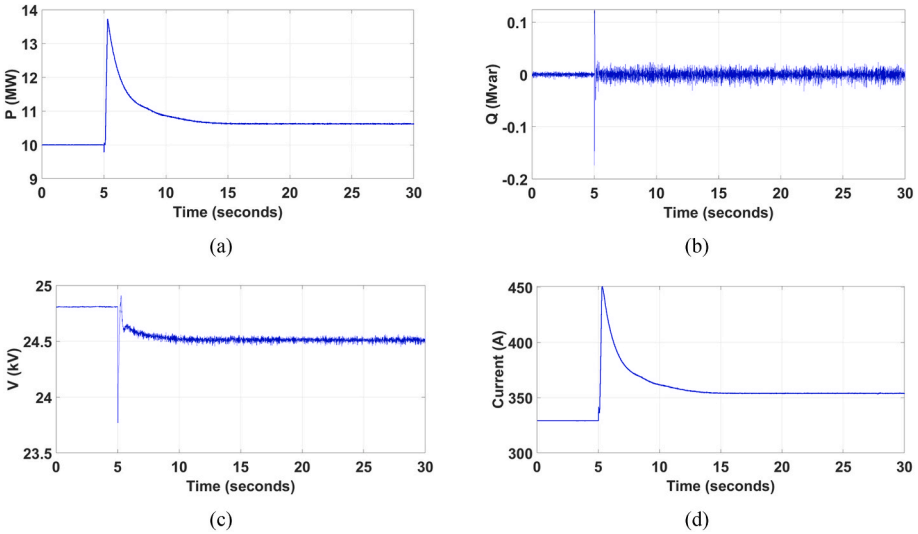

Fig. 8. Response of the LAES against microgrid disconnection (a) active power response (b) reactive power response (c) voltage at the access point (d) Current waveform response of the LAES.

compared to other energy storage technologies. When the LAES is controlled more adaptively, e.g., the proposed Fuzzy control case in this paper, the fast frequency response performance becomes much better. The Fuzzy based control of LAES combined with the inertia terms of WT-BESS has yielded the best frequency nadir improvement of 59.974 Hz, a significant improvement compared with all other cases. It is notable that when none of the connected renewable sources participate in the fast frequency response, the microgrid frequency nadir is the lowest, which may cause the system to collapse if the load is not shed. Also, in most of the control schemes, at first the frequency improved but later caused a worse SFD. This effect is presented in Fig. 6 (b). Such a large SFD jeopardizes the stability of the system. Therefore, it is very important to provide a control scheme, capable of keeping the frequency within the statutory limits. In this context, the proposed Fuzzy-combined approach has been effective to improve the frequency nadir, significantly better than the other 27 fixed gain schemes.

In the next scenario, the load demand is set to the high and severe case of 52 MW. The system frequency is at the nominal value of 60 Hz while the microgrid is connected to the upstream grid. At t = 5s, the microgrid is disconnected. The same control schemes are applied to observe their performance in presence of a more severe power mismatch.

The high magnitude of the load demand causes frequency collapse if no frequency control is performed from the hybrid RES. Also, the clusters of cases 4–6, cases 13–15 and cases 22–24 failed to maintain the frequency stability as a result of their severe SFDs. Given the dynamical complexity of LAES and yet its efficiency to provide ancillary service, the proposed Fuzzy control scheme is applied to allow a more flexible control response. The main aim of the proposed Fuzzy controller is to improve the frequency nadir and keep it within the statutory limits. As it is seen from Fig. 10, the FFR performance of the Fuzzy control-based scenario is much better, while some other cases failed to keep the stability of the system. The cases 7–9 also provided an acceptable and robust frequency response to stabilize the system.

4.2. Experimental results

The performance of the control scheme on the hybrid LAES-WT-BESS

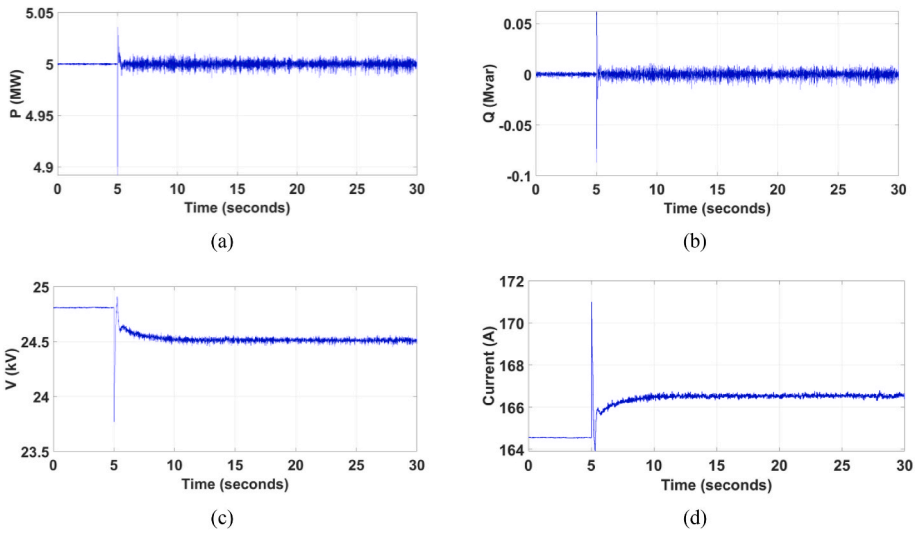

Fig. 9. Response of the BESS against microgrid disconnection (a) active power response (b) reactive power response (c) voltage at the access point (d) Current waveform response of the BESS.

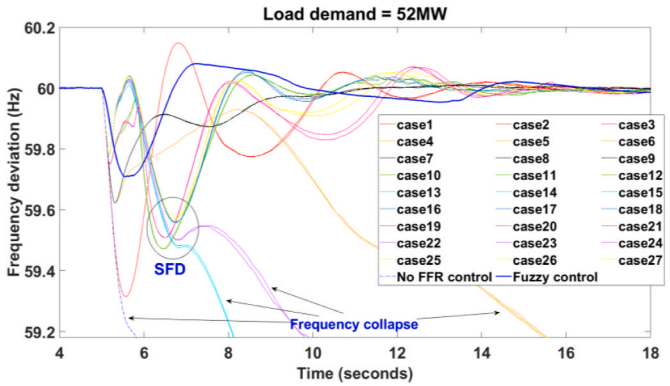

Fig. 10. Fast Frequency Response Control in the hybrid RES microgrid with higher load demand.

is validated using the real-time Opal-RT Hardware-in-loop test rig, shown in Fig. 11. The microgrid is modelled in RT-LAB. One grid emulator and three load emulators have been used to emulate the performance of the grid, WT, LAES and BESS. The data transmission between the real-time simulator and the emulators is operated over Modbus communication protocol. The overall stable performance of the system is shown in Fig. 12. The voltage level at the microgrid busbar remains stable and the injected power by the LAES emulator, the WT emulator, and the BESS emulator to the microgrid busbar follow the command signals of the developed FFR controller, sent from the real-time simulator. Superposition of the injected powers from these emulators counterbalance the power mismatch in the microgrid system which was a result of grid disconnection and the power imbalance between RES generations and load.

5. Discussion

The UK electricity system operator has an obligation to control system frequency at 50Hz within the narrow range of ± 0.5 Hz. While, the UK electricity system is planned to be decarbonised by 2035, the costs regarding the frequency containments may increase with the growth in the shares of intermittent renewable sources. The total spent to balance the electricity system for the month of July 2022 alone was £333.52 m in which £89.81 m spent on ancillary services [43]. From the economic perspective, the proposed control strategy utilizes LAES as a more predictable and reliable source of energy to provide multi-time scale renewable-based ancillary service and results in lowering the operational costs and spinning reserves, hence, decreasing costs to the consumers.

The proposed hybrid LAES-based ancillary service system leads to effective investment choices that may help build a more robust system. A comprehensive analysis of the fast frequency response of the hybrid LAES-WT-BESS system was conducted. The inertial control term, droop control term as well as both inertial and droop controls were applied on each of these three resources, forming 27 scenarios. The performance of these control actions can be sorted into 9 different groups, which are marked with different colours in Fig. 6. For example, cases 7, 8 and 9 which are marked in black in Fig. 6 (a), performed similarly, dominated by the contribution of LAES. This group mitigated the frequency nadir to 59.754 Hz, and had better overall performance compared with other groups. The other cases suffered from SFD or severe frequency nadir. Cases 1-3 marked in red, resulted in the worst frequency nadir, while the cases 13–15 (cyan), cases 16–18 (blue), cases 22–24 (purple) and cases 25–27 (yellow) imposed severe SFD to the system. Cases 4, 5 and 6

Fig. 11. The real-time hardware-in-the-loop experimental test validations.

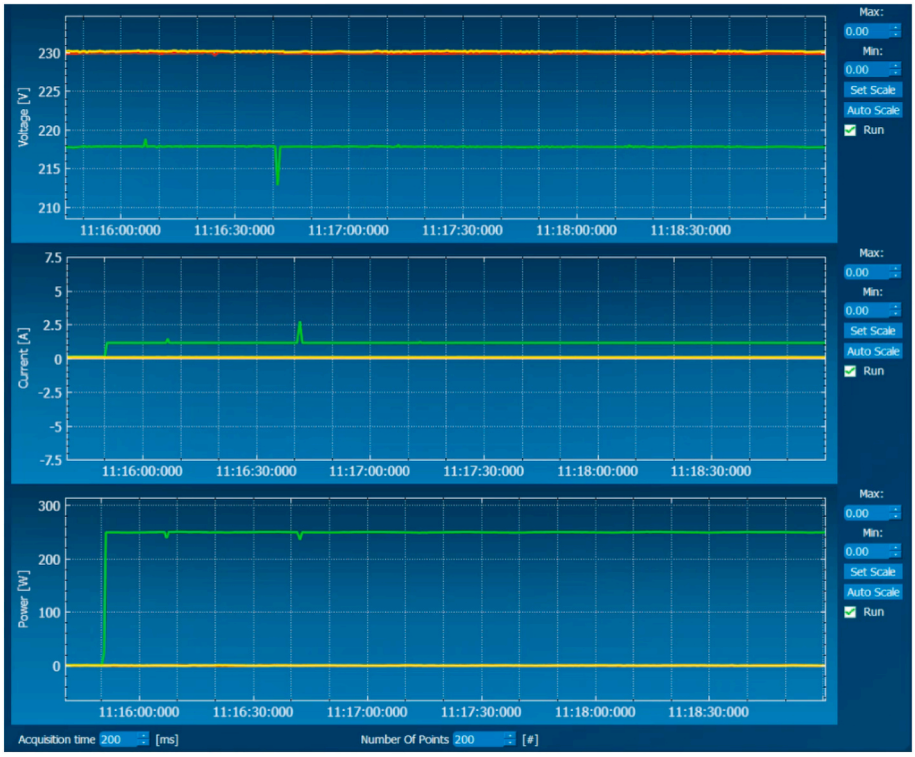

Fig. 12. The stable performance of the emulators at the experimental test.

shown in orange, showed an acceptable performance against 50 MW load disturbance as shown in Fig. 6. However, this group had frequency control failure against 52 MW scenario shown in Fig. 10. The group marked in black provided a reliable FFR against different load changes. To further improve the frequency nadir against different disturbances, the Fuzzy control was used to control the output power of the LAES more flexibly along with the inertial control of WT and BESS systems.

It is vital to effectively store energy from the variable RES. Taking the UK as an example, in the past two years, 5.8 TWh of UK's wind power was curtailed and wasted at the cost of £806 million, due to the transmission network congestion and lack of long-duration storage capacity, enough to supply 800,000 homes a year [44]. The curtailment costs would increase along with the growth of the share of offshore wind farms in next few years. LAES could provide significant support to avoid curtailments and provide constraints managements. Furthermore, technologies such as LAES would help the UK realize its pledge to be carbon neutral by 2050. The suggested renewable supported LAES system is fully environmentally-friendly since it only uses the excess power of RES for the compression phase, as well as running a renewable-based combustion chamber [45].

The surplus generated power of the intermittent RES can be stored as liquefied air to be used during the peak demands, contingencies or balancing services [46,47]. The stored liquid air has the advantage to be used as seasonal storage or on-demand source to the grid for power system frequency control. Furthermore, in future works, the focus will be on developing an advanced intelligent control algorithm for the hybrid LAES-Wind system to provide ancillary service with optimal RES inputs in a large-scale power system in presence of dynamical load changes, wind uncertainties, disturbances, noise, and model uncertainties. In this regards, advanced storage models that incorporate off-design performance, technological restrictions to LAES operation such as viable power modulation regions, ramp rates, and other non-idealities, as well as frameworks to integrate these LAES models in system-level evaluation, are required and considered [48,49].

6. Conclusion

LAES is an emerging technology that could help with integration of renewable energy sources, in particular offshore wind farms. An overall assessment of the fast frequency response of hybrid LAES-WT-BESS system was conducted using inertial, droop and fuzzy control systems. Of different control strategies, the WT and the BESS were equipped with inertial control, while a Fuzzy control system was assigned to the LAES. This control scheme resulted in a better frequency nadir improvement compared with other frequency control schemes. When designing a fast frequency response scheme, it is important to consider dynamical changes to the system. To enhance the capabilities of hybrid renewable energy sources, variable control gains, adaptable to the changes in the system, results in a better control action. Although the research on the ancillary services of LAES is currently at its early stage, it is recommended to implement adaptive and flexible control approaches more suitable with the dynamics of the complex power system.

Declaration of competing interest

The authors declare that they have no known competing financial interests or personal relationships that could have appeared to influence the work reported in this paper.

Acknowledgements

This work was supported by the UK Engineering and Physical Sciences Research Council under grant numbers: EP/S000747/1 and EP/S032622/1.

References

[1] Department for Business, Energy & Industrial Strategy "Early phase out of unabated coal generation in Great Britain: government response, Available at: https://www.gov.uk/government/consultations/early-phase-out-of-unabated-coal-generation-in-great-britain#documents, Dec 2020.

[2] Department for Business, Energy & Industrial strategy "British energy security strategy" 7 april 2022, Available at: https://www.gov.uk/government/publications/british-energy-security-strategy/british-energy-security-strategy.

[3] C. Wang, Q. Cui, Z. Dai, et al., Performance analysis of liquid air energy storage with enhanced cold storage density for combined heating and power generation, J. Energy Storage 46 (Feb 2022), 103836.

[4] IEA, Renewable energy market update. https://www.iea.org/reports/renewable-energy-market-update-2021, 2021. (Accessed 11 July 2022).

[5] C.A. Agostini, F.A. Armijo, C. Silva, S. Nasirov, The role of frequency regulation remuneration schemes in an energy matrix with high penetration of renewable energy, Renew. Energy 171 (2021) 1097–1114.

[6] M. Kheshti, L. Ding, M. Nayeripour, X. Wang, V. Terzija, Active power support of wind turbines for grid frequency events using a reliable power reference scheme, Renew. Energy 139 (2019) 1241–1254.

[7] A. Vecchi, Y. Li, Y. Ding, P. Mancarella, A. Sciacovelli, Liquid air energy storage (LAES): a review on technology state-of-the-art, integration pathways and future perspectives, Advances in Applied Energy 3 (2021), 100047.

[8] D. Graf, J. Marschewski, L. Ibing, et al., What drives capacity degradation in utility-scale battery energy storage systems? The impact of operating strategy and temperature in different grid applications, J. Energy Storage (2022), https://doi.org/10.1016/j.est.2021.103533.

[9] A. Benmouna, M. Becherif, L. Boulon, C. Dépature, H.S. Ramadan, Efficient experimental energy management operating for FC/battery/SC vehicles via hybrid Artificial Neural Networks-Passivity Based Control, Renew. Energy 178 (2021) 1291–1302.

[10] M.S. Javed, T. Ma, J. Jurasz, M.Y. Amin, Solar and wind power generation systems with pumped hydro storage: review and future perspectives, Renew. Energy 148 (2020) 176–192.

[11] J. Yuan, X. Luo, Z. Li, L. Li, P. Ji, Q. Zhou, Z. Zhang, Sustainable development evaluation on wind power compressed air energy storage projects based on multi-source heterogeneous data, Renew. Energy 169 (2021) 1175–1189.

[12] G.L. Guizzi, M. Manno, L.M. Tolomei, R.M. Vitali, G. Leo Guizzi, M. Manno, et al., Thermodynamic analysis of a liquid air energy storage system, Energy 93 (2015) 1639–1647, https://doi.org/10.1016/j.energy.2015.10.030.

[13] Xue XD, Wang SX, Zhang XL, Cui C, Chen LB, Zhou Y, et al. Thermodynamic Analysis of a Novel Liquid Air Energy Storage System. *Phys Procedia* n.d.;67: 733–738. https://doi.org/10.1016/j.phpro.2015.06.124.

[14] X. She, X. Peng, B. Nie, G. Leng, X. Zhang, L. Weng, et al., Enhancement of round trip efficiency of liquid air energy storage through effective utilization of heat of compression, Appl. Energy 206 (2017) 1632–1642, https://doi.org/10.1016/j.apenergy.2017.09.102.

[15] X. Peng, X. She, Y. Li, Y. Ding, Thermodynamic analysis of liquid air energy storage integrated with a serial system of organic rankine and absorption refrigeration cycles driven by compression heat, Energy Proc. 142 (2017) 3440–3446, https://doi.org/10.1016/j.egypro.2017.12.227.

[16] A.Z. Al Shaqsi, K. Sopian, A. Al-Hinai, Review of energy storage services, applications, limitations, and benefits, Energy Rep. 6 (2020) 288–306, https://doi.org/10.1016/j.egyr.2020.07.028.

[17] H. Guo, Y. Xu, X. Zhang, Q. Liang, S. Wang, H. Chen, Dynamic characteristics and control of supercritical compressed air energy storage systems, Appl. Energy 283 (2021), 116294, https://doi.org/10.1016/j.apenergy.2020.116294.

[18] S. Cui, Q. He, X. Shi, Y. Liu, D. Du, Dynamic characteristics analysis for energy release process of liquid air energy storage system, Renew. Energy 180 (2021) 744–755, https://doi.org/10.1016/j.renene.2021.08.115.

[19] S. Cui, C. Lu, X. Shi, D. Du, Q. He, W. Liu, Numerical investigation of dynamic characteristics for expansion power generation system of liquefied air energy storage, Energy 226 (2021), 120372, https://doi.org/10.1016/j.energy.2021.120372.

[20] C. Lu, Q. He, S. Cui, X. Shi, D. Du, W. Liu, Evaluation of operation safety of energy release process of liquefied air energy storage system, Energy 235 (2021), 121403, https://doi.org/10.1016/j.energy.2021.121403.

[21] P. Zhao, M. Wang, J. Wang, Y. Dai, A preliminary dynamic behaviors analysis of a hybrid energy storage system based on adiabatic compressed air energy storage and flywheel energy storage system for wind power application, Energy 84 (2015) 825–839, https://doi.org/10.1016/j.energy.2015.03.067.

[22] S. Cui, J. Song, T. Wang, Y. Liu, Q. He, W. Liu, Thermodynamic analysis and efficiency assessment of a novel multi-generation liquid air energy storage system, Energy 235 (2021), 121322, https://doi.org/10.1016/j.energy.2021.121322.

[23] A. Vecchi, Y. Li, P. Mancarella, A. Sciacovelli, Integrated techno-economic assessment of Liquid Air Energy Storage (LAES) under off-design conditions: links between provision of market services and thermodynamic performance, Appl. Energy 262 (2020), https://doi.org/10.1016/j.apenergy.2020.114589.

[24] Y. Du, Y. Yang, D. Hu, M. Hao, J. Wang, Y. Dai, Off-design performance comparative analysis between basic and parallel dual-pressure organic Rankine cycles using radial inflow turbines, Appl. Therm. Eng. 138 (2018) 18–34, https://doi.org/10.1016/j.applthermaleng.2018.04.036.

[25] N.H. Samrat, N Bin Ahmad, I.A. Choudhury, Z Bin Taha, Modeling, control, and simulation of battery storage photovoltaic-wave energy hybrid renewable power generation systems for island electrification in Malaysia, Sci. World J. 2014 (2014), https://doi.org/10.1155/2014/436376.

[26] R.A. Biroon, P. Pisu, D. Schoenwald, Large-scale Battery Energy Storage System Dynamic Model for Power System Stability Analysis, IEEE Texas Power Energy Conf TPEC, 2020, https://doi.org/10.1109/TPEC48276.2020.9042536, 2020.

[27] Z. Liu, D. Kim, T. Gundersen, Optimal recovery of thermal energy in liquid air energy storage, Energy 240 (2022), 122810.

[28] C. Damak, D. Leducq, H.M. Hoang, D. Negro, A. Delahaye, Liquid air energy storage (LAES) as a large-scale storage technology for renewable energy integration - a review of investigation studies and near perspectives of LAES, Int. J. Refrig. 110 (2020) 208–218.

[29] E. Borri, A. Tafone, A. Romagnoli, G. Comodi, A preliminary study on the optimal configuration and operating range of a "microgrid scale" air liquefaction plant for Liquid Air Energy Storage, Energy Convers. Manag. 143 (2017) 275–285.

[30] C. Xie, Y. Hong, Y. Ding, Y. Li, J. Radcliffe, An economic feasibility assessment of decoupled energy storage in the UK: with liquid air energy storage as a case study, Appl. Energy 225 (2018) 244–257.

[31] A. Vecchi, J. Naughton, Y. Li, P. Mancarella, A. Sciacovelli, Multi-mode operation of a Liquid Air Energy Storage (LAES) plant providing energy arbitrage and reserve services e Analysis of optimal scheduling and sizing through MILP modelling with integrated thermodynamic performance, Energy 200 (2020), 117500.

[32] G.A.M. Tirantha Bandara, S. Rajakaruna, A. Ghosh, Evaluating of frequency response time characteristics of large scale energy storage systems in high renewable energy penetrated power systems, in: 31st Australasian Universities Power Engineering Conference (AUPEC), Sept. 2021, pp. 26–30. Perth, Australia.

[33] X. Peng, X. She, L. Cong, T. Zhang, C. Li, Y. Li, L. Wang, L. Tong, Y. Ding, Thermodynamic study on the effect of cold and heat recovery on performance of liquid air energy storage, Appl. Energy 221 (2018) 86–99, https://doi.org/10.1016/j.apenergy.2018.03.151.

[34] O. O'Callaghan, P. Donnellan, Liquid air energy storage systems: a review, Renew. Sustain. Energy Rev. 146 (August 2021), 111113.

[35] P.M. Anderson, M. Mirheydar, A Low-order system frequency response model, IEEE Trans. Power Syst. 5 (3) (Aug. 1990) 720–729.

[36] M. Kheshti, L. Ding, W. Bao, M. Yin, Q. Wu, V. Terzija, Toward intelligent inertial frequency participation of wind farms for the grid frequency control, IEEE Trans. Ind. Inf. 16 (11) (2020) 6772–6786, Nov.

[37] J. Van de Vyver, J.D.M. De Kooning, B. Meersman, L. Vandevelde, T.L. Vandoorn, Droop control as an alternative inertial response strategy for the synthetic inertia on wind turbines, IEEE Trans. Power Syst. 31 (2) (March 2016) 1129–1138.

[38] W. Bao, L. Ding, Z. Liu, et al., Analytically derived fixed termination time for stepwise inertial control of wind turbines—Part I: analytical derivation, Int. J. Electr. Power Energy Syst. 121 (2020) 1–10.

[39] Y. Guo, W. Bao, L. Ding, et al., "Analytically derived fixed termination time for stepwise inertial control of wind turbines—Part II: application strategy," Int. J. Electr. Power Energy Syst., vol. 121, 2020.

[40] M. Hwang, E. Muljadi, G. Jang, Y.C. Kang, Disturbance-adaptive short-term frequency support of a DFIG associated with the variable gain based on the ROCOF and rotor speed, IEEE Trans. Power Syst. 32 (3) (2017) 1873–1881.

[41] M. Altin, A.D. Hansen, T.K. Barlas, et al., Optimization of short-term overproduction response of variable speed wind turbines, IEEE Trans. Sustain. Energy 9 (4) (2018) 1732–1739.

[42] M. Kheshti, S. Lin, X. Zhao, et al., Gaussian distribution-based inertial control of wind turbine generators for fast frequency response in low inertia systems, IEEE Trans. Sustain. Energy 13 (3) (2022) 1641–1653.

[43] E.S.O. National Grid, Monthly Balancing Services Summary 2022/23 June 2022, June 2022.

[44] Renewable Curtailment and the Role of Long Duration Storage" *LCP Report for Drax*, May 2022.

[45] M. Nabat, M. Soltani, A. Razmi, et al., Investigation of a green energy storage system based on liquid air energy storage (LAES) and high-temperature concentrated solar power (CSP): energy, exergy, economic, and environmental (4E) assessments, along with a case study for San Diego, US, Sustain. Cities Soc. 75 (December 2021), 103305.

[46] M. Yang, L. Duan, Y. Tong, Y. Jiang, Study on design optimization of new liquified air energy storage (LAES) system coupled with solar energy, J. Energy Storage 51 (July 2022), 104365.

[47] Y. Cao, S. Mousavi, P. Ahmadi, Techno-economic assessment of a biomass-driven liquid air energy storage (LAES) system for optimal operation with wind turbines, Fuel 324 (15 September 2022), 124495. Part B.

[48] T. Liang, T. Zhang, Y. Li, et al., Thermodynamic analysis of liquid air energy storage (LAES) system, Encyclopedia of Energy Storage 1 (2022) 232–252.

[49] M. Qi, J. Park, I. Lee, I. Moon, Liquid air as an emerging energy vector towards carbon neutrality: a multi-scale systems perspective, Renew. Sustain. Energy Rev. 159 (2022), 112201.